Collective modes and superconductivity in an extended Hubbard model for copper oxide superconductors

P. B. Littlewood
AT&T Bell Laboratories, Murray Hill, New Jersey 07974-2070
(Received 11 August 1989; revised manuscript received 31 August 1990)

A three-band extended Hubbard model for CuO_2 planes is explored within a self-consistent-field approximation. The collective modes for both charge and spin fluctuations are calculated, including leading-order self-energy corrections for the quasiparticle propagators; this leads to an approximate form for the renormalized quasiparticle interactions, used to study superconductive pairing. We find that spin fluctuations promote pairing of B_{1g} symmetry ($d_{x^2-y^2}$), and charge fluctuations between Cu and O induce either A_{1g} (extended s) or B_{2g} (d_{xy}) pairing.

I. INTRODUCTION

Since the discovery[1] of high-temperature superconductivity in the copper oxide compounds, an innumerable variety of electronic mechanisms have been proposed. Many of the models are based, either in detail, or in spirit, on the two-dimensional Hubbard model for a square lattice of CuO_2. The most general form for such a model Hamiltonian includes both Cu and O planar orbitals as well as onsite and intersite Coulomb repulsion. Depending upon the parameters of the model, either spin or charge fluctuations may be the dominant features.

In this paper we present the details of a self-consistent-field approach to this problem, which has the advantage of treating spin and charge fluctuations on an equal footing, so that we may dissect the resulting interactions to study the independent influence of these fluctuations on superconductive pairing. Our approach is straightforwardly generalizable to models with more complex band structure, and longer-range interactions. These calculations have validity restricted in principle to weak coupling, and to a Fermi-liquid ground state. Nevertheless, we believe that they provide a good indication of the general features to be expected in a regime of stronger interactions; comparison of the present self-consistent-field results to those of a Gutzwiller variational wave function shows that all essential qualitative features are present in both approaches.[2] A strength of the present approach is that the results have a straightforward physical interpretation, and the subtle effects associated with local-field corrections are made manifest. Some preliminary results have been presented elsewhere.[3,4]

This paper also addresses many of the issues which were raised some time ago concerning earlier models for excitonic superconductivity.[5-9] The model of Allender, Bray, and Bardeen[5] (ABB) involved a direct (Coulombic) coupling to transverse excitonic modes, which was criticized by Inkson and Anderson[7] (IA) for the failure to treat correctly the long-range Coulomb interaction; this guarantees repulsion at low frequencies and apparently allows attractive interactions mediated only by the exchange of *longitudinal* plasmons. Whether or not plasmons can yield an attractive BCS kernel has been a subject of some controversy, with a Lindhard form for the dielectric function leading to a *repulsive* interaction.[8] However, a model dielectric function used by IA (Ref. 7) and others does lead to attraction at moderate frequencies.[8] The difference between these calculations suggests that one must pay particular care to the momentum dependence of the interaction. In any case, it is clear that the static interaction is repulsive, and any pairing obtained in the BCS approximation is unlikely to survive the large self-energy and vertex corrections.[9]

A different question concerns the possible coupling to transverse excitonic modes via *umklapp* processes, or local-field corrections, which was implicit in ABB, and subsequently articulated more carefully.[6] IA concluded that local-field corrections would be small and of no help, apparently because they subsumed the off-diagonal elements of the dielectric matrix into a correction to the long-wavelength dielectric constant. However, as stressed by Cohen and Louie,[8] this is only a partial answer; it ignores the short-range parts of the interaction except as they modify the longer-range screening. A full treatment of the local-field corrections demands a detailed calculation, which was apparently never performed for the model of ABB, and the questions raised there remain open. For the model we shall consider, the local-field corrections are crucial to obtain superconductivity.

We use a Hamiltonian for the CuO_2 planes in a tight-binding basis, which is an extended Hubbard model defined on the $d_{x^2-y^2}$ orbital for Cu and the (σ) p_x orbital on one of the two O atoms in the unit cell and the (σ) p_y orbital on the other:[10]

$$H=\epsilon\sum_i(c_{di}^\dagger c_{di}-c_{xi}^\dagger c_{xi}-c_{yi}^\dagger c_{yi})+\sum_{\langle ij\rangle}[(t_{ij}c_{di}^\dagger c_{xj}+\text{H.c.}+(x\rightarrow y)]+\sum_{\langle ij\rangle}(t'_{ij}c_{xi}^\dagger c_{yj}+\text{H.c.})$$
$$+\tfrac{1}{2}U\sum_i \delta n_{di}\,\delta n_{di}+\tfrac{1}{2}U_p\sum_i[\delta n_{xi}\,\delta n_{xi}+(x\rightarrow y)]+V\sum_{\langle ij\rangle}\delta n_{di}(\delta n_{xj}+\delta n_{yj})\ . \quad (1)$$

Here, $\epsilon=\frac{1}{2}(E_d-E_p)$, $t_{ij}=\pm t$, and we have included a repulsive U on Cu and O as well as the nearest-neighbor repulsive V. All energy parameters will be given in units scaled by t. The notation $\langle ij \rangle$ specifies nearest-neighbor summation, and we have both a direct Cu-O overlap t, as well as a nearest-neighbor O-O overlap t'. The band parameters ϵ and t are defined in the Hartree-Fock approximation, and $\delta n_i=n_i-\langle n_i \rangle$. The band filling is written as $n=\frac{1}{2}(1-\delta)$, and δ will be referred to as the hole concentration, although this nomenclature has no particular significance for the Fermi liquid.

There have been a number of attempts to estimate or calculate the various parameter values in this Hamiltonian, with generally good agreement.[11] These estimates are in the following ranges: $U_d \sim 8-10$ eV, $U_p \sim 3-6$ eV, $V \sim 1-1.5$ eV, $t \sim 1.5$ eV, $t' \sim 0.5$ eV, and $\epsilon \sim 0$. Note that the value of ϵ in our calculation is the *renormalized* Hartree-Fock value, which is assumed small, close to the value obtained in band-structure calculations.[11,12] The bare value of ϵ is somewhat larger.[2] In our calculations, we shall use somewhat smaller values of U than generally accepted. This is for purely technical reasons, in order that the metallic state be stable within our calculational scheme. Furthermore, although it is straightforward to include U_p in our approach, we find that it is not a crucial parameter (provided that $U_p < U$), and to simplify the presentation we shall neglect the on-site oxygen interaction in most cases.

The single-band Hubbard model has been extensively analyzed in a weak-coupling expansion[13,14] and by Monte Carlo methods.[15] The comparison of these two approaches shows that at least at moderate energies, a perturbation expansion for intermediate coupling is reasonable.[16] The multiband Hubbard model has also been treated within a variational Gutzwiller approach,[17] numerical diagonalization of small clusters,[18] slave boson techniques,[19] Monte Carlo,[20] and other methods.[21-23] A recent calculation by Wagner *et al.*[24] employs both strong- and weak-coupling techniques; the weak-coupling results are directly comparable to ours.

We find that the three-band model does not differ substantially from the single-band case, provided that the interatomic Coulomb interaction (V) is small. Close to half-filling the system will be a Mott-Hubbard antiferromagnetic insulator, and these calculations are not appropriate for the ground-state properties, although they do, of course, indicate the instability to an insulating antiferromagnet through a spin-density-wave (SDW) transition.

If there are sizable charge fluctuations, however, the picture is more complex, and a single-band model is generally no longer adequate. Even at half-filling, the lowest energy charge fluctuations involve charge transfer between Cu and O sites.[25] Such transitions will be modified by the effect of the intersite Coulomb interaction V and may lead to a localized (but optically forbidden) "exciton"; with doping away from half-filling this feature will broaden into a charge-transfer resonance (CTR). For strong enough intersite coupling, the CTR contains the dominant fluctuations in the charge channel. In order to capture the physics of these and other charge fluctuations correctly, it is necessary to allow for localized fluctuations within a unit cell. Calculations that treat these local-field effects improperly may give spurious results. In particular, charge fluctuations will induce competing repulsive and attractive interactions in different channels; the balance between attraction and repulsion is very delicate. Charge fluctuations naturally give rise to attraction between quasiparticles on the oxygen sites;[23] however, the repulsion V between carriers on O and Cu is, in fact, enhanced,[4] so that the existence of a superconductive ground state remains uncertain without a detailed calculation incorporating the effects of hybridization. This competition exists even if the charge fluctuations are themselves primarily *intra*band in nature [for example, in the vicinity of a charge-density-wave (CDW) transition]. Furthermore, we find that although intraband charge fluctuations may soften, the range of momenta where such modes are of low energy is small; we find an incipient CDW is an ineffective promotor of superconductivity, unlike some other work.[26]

In contrast, charge-transfer excitations (i.e., between copper and oxygen), as suggested previously,[10] are more effective for inducing pairing. Provided only that the charge-transfer-resonance modes are at an energy of the order of the conduction bandwidth, or lower, we find a moderate transition temperature for (extended) s-wave pairing. Such a result is indicated by other calculations, both within weak[24,27] and strong[18,19,21,24] coupling. However, it is very important to distinguish superconductive pairing from other instabilities, such as phase separation of the holes[21,28] or a CDW transition. One must check that the metallic state is stable in the *particle-hole* channel, before investigating superconductivity. Some of the calculations do not include the local-field effects,[19,27] without which we do not find pairing.

In this paper we shall be concerned with understanding the effects of these fluctuations (both charge and spin) on both the single-particle and two-particle properties in the metallic state. The outline follows.

In Sec. II we exhibit the formalism for our calculations, with some details relegated to an Appendix. This comprises, first, a solution of the particle-hole T matrix to obtain the collective modes in both the charge and spin channel; second, this procedure generates automatically renormalized interactions between quasiparticles; third and finally, these interactions are inserted into the gap equations for superconductivity. These calculations may be performed either with or without self-energy corrections to the quasiparticle propagators. The separation between particle-hole and particle-particle channels made here is a good approximation, provided that $T_c/t \ll 1$.[29]

In Sec. III we present detailed numerical results. We find that the metallic state may be unstable in the particle-hole channel in three possible ways:[3]

(i) A SDW instability, promoted by the on-site Coulomb interactions and determined in weak coupling by only intraband interactions; (ii) a CDW instability, also involving intraband interactions, but in this case driven by the intersite repulsion; (iii) the softening of the CTR, which is again driven by V, but is a $\mathbf{q} \sim 0$ phenomenon involving interband processes.

Phase separation would be indicated by a negative compressibility $dn/d\mu$ in the static limit, which is easily checked within the static limit of our approach (i.e., Hartree-Fock). We find the compressibility positive for all parameters such that the CTR is stable.[2] However, the local charge fluctuations corresponding to the CTR do couple to the compressibility. Consequently, the charge-transfer instability (CTI) coincides with phase separation, and is, in fact, the driving force for phase separation in this approximation. The cluster calculations that have shown phase separation[28] have been performed for parameters very different from those we have used. In particular, these calculations used *bare* values of $\epsilon \sim 0$, whereas it is the *renormalized p-d* splitting that is believed close to zero.[11]

A technical feature of our calculation is that we shall choose to fix the physical renormalized value ϵ, rather than the bare parameter ϵ_0. Because the CTI is a first-order transition, and the two-phase region corresponds to two different values of ϵ consistent with the same ϵ_0,[2] it is necessary to be sure that one is in the stable (rather than metastable) phase. This is the case for all parameter values discussed here; further discussion of the parameter space is given elsewhere.[2]

The SDW and CDW instabilities are sensitive to details of the band structure and, in particular, to the "nesting" of the Fermi surface near half-filling. The inclusion of self-energy corrections suppresses both the CDW and SDW instabilities, and the dominant charge fluctuation mode is the CTR.[3] The CTI is, in general, a *first*-order transition between two locally stable values of the relative Cu and O occupancy. As we shall here work with parameters that hold the relative occupancies fixed, since they are largely determined by Coulomb interaction with ions outside the two-dimensional (2D) layer, we shall find only a soft-mode transition, which corresponds to a critical point in a Hartree-Fock theory with the bare parameters fixed. This is discussed in more detail in Ref. 2.

We also discuss the way that these fluctuations renormalize the single-particle spectrum, particularly in the vicinity of the SDW phase boundary. The influence of these different fluctuations on superconductive pairing can be dissected by separating the intraband and interband contributions to the effective interaction. In Sec. IV we discuss the general applicability of these results, as compared with other approaches.

II. MODEL

In order to determine the collective modes in the metallic phase, we begin with the Bethe-Salpeter equation for the particle-hole T matrix, shown diagrammatically in Fig. 1(a). The bare interaction [Fig. 1(b)] includes both direct and exchange terms, and, unlike the simple case of the single-band Hubbard model,[30] the inclusion of intersite interactions and multiple orbitals leads to a momentum-dependent interaction and an integral equation for the effective interaction Γ. The trick which enables a rapid numerical solution of this equation is that the interactions may be written in a factorizable form[31]

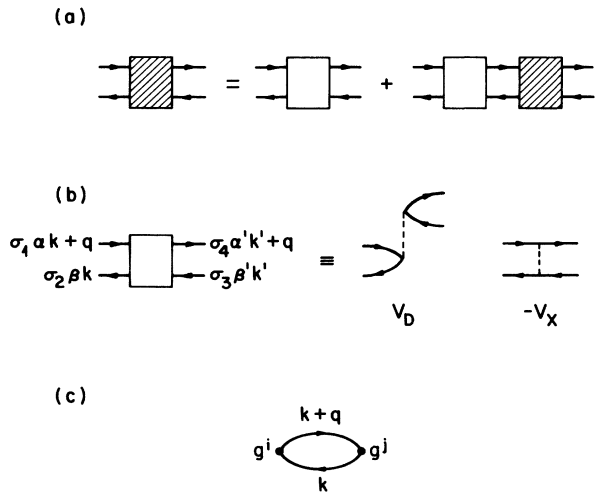

FIG. 1. Bethe-Salpeter equation for the (a) effective particle-hole interaction Γ with the (b) bare interaction and the (c) polarizability.

by introducing a set of particle-hole basis functions g^i, so that

$$V(\sigma_1,\alpha,\mathbf{k}+\mathbf{q};\sigma_2,\beta,\mathbf{k};\sigma_3,\beta',\mathbf{k}';\sigma_4,\alpha',\mathbf{k}'+\mathbf{q}) = \sum_{i,j} g^i_{\alpha\beta}(\mathbf{k},\mathbf{k}+\mathbf{q}) g^j_{\alpha'\beta'}(\mathbf{k}',\mathbf{k}'+\mathbf{q}) \times [V^{ij}_\rho(\mathbf{q},\omega)\delta_{1,2}\delta_{3,4} + V^{ij}_\sigma(\mathbf{q},\omega)\boldsymbol{\sigma}_{1,2}\cdot\boldsymbol{\sigma}_{3,4}] . \quad (2)$$

Here $\alpha,\beta,\ldots$ refer to orbitals, and the subscripts in Roman numerals are spin indices. The effective interaction Γ has an identical form to Eq. (2). In the present case, it is convenient to use an 11-component basis set; this is given in the Appendix, along with the matrices V^{ij}.

In Eq. (2) we have also separated the interaction into charge ($V_\rho = \frac{1}{2}[2V_D - V_X]$) and spin ($V_\sigma = -\frac{1}{2}V_X$) channels. The integral equation for the T matrix now reduces to the solution of the 11×11 matrix equations:

$$\Gamma_{\rho,\sigma} = [1 - 2V_{\rho,\sigma}P]^{-1} V_{\rho,\sigma} , \quad (3)$$

where we have suppressed the indices and q [$\equiv(\mathbf{q},\omega)$] dependence for clarity. Here, $P^{ij}(\mathbf{q},\omega)$ is the particle-hole polarizability in the basis of the g's [see Fig. 1(c)]:

$$P^{ij}(q) = \sum_{\alpha,\alpha',\beta,\beta'} \sum_p g^i_{\alpha\beta}(\mathbf{p}+\mathbf{q},\mathbf{p}) G_{\alpha\alpha'}(p+q) \times G_{\beta'\beta}(p) g^i_{\alpha'\beta'}(\mathbf{p}+\mathbf{q},\mathbf{p}) . \quad (4)$$

Equation (3) generates the effective interactions, as well as determining the particle-hole collective modes as zeros of the eigenvalue equation:

$$[\chi_{\rho,\sigma}(q)]\psi^{(k)} = [1 - 2V_{\rho,\sigma}(\mathbf{q})P(q)]\psi^{(k)} = \lambda^{(k)}_{\rho,\sigma}(q)\psi^{(k)} , \quad (5)$$

where the superscript (k) labels the kth eigenvector. χ is the generalized nonlocal spin and charge susceptibility, and includes the full local-field corrections for the model. The collective mode dispersion relation is determined by

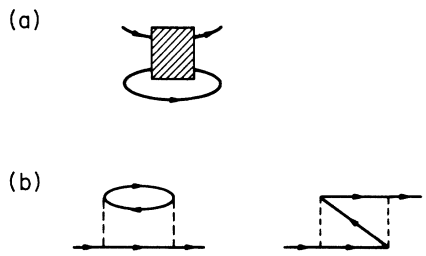

FIG. 2. Quasiparticle self-energy (a) from the full T matrix, and (b) to second order in the interactions.

$$\lambda^{(k)}(\mathbf{q},\omega_q^{(k)})=0 .$$

The effective interactions may also be used to renormalize the quasiparticle propagators by means of self-energy effects [see Fig. 2(a)], leading to

$$\Sigma_{\alpha\alpha'}(k)=\sum_{i,j,q,\beta,\beta'} g^i_{\alpha\beta}(\mathbf{k},\mathbf{k}-\mathbf{q}) \times g^j_{\alpha'\beta'}(\mathbf{k},\mathbf{k}-\mathbf{q})G_{\beta\beta'}(k-q) \times[\Gamma^{ij}_\rho(q)+3\Gamma^{ij}_\sigma(q)] . \quad (6)$$

Replacing Γ in Eq. (6) by the bare interactions V yields the Hartree-Fock approximation, which we have included already in the definition of the Hamiltonian [Eq. (1)]; thus the bare interaction terms must be subtracted out. In practice, we shall often use only terms up to the second order in the interactions [see Fig. 2(b)]; these are the leading terms that generate a finite lifetime for quasiparticles away from the Fermi surface.

We now take a conventional approach to the superconducting behavior by using the effective interaction Γ [Eq. (3)] as the bare interaction in the particle-particle channel. Solution of the particle-particle T-matrix equation leads to the equation for the gap function at T_c, which is

$$\phi_{\alpha\beta}(\mathbf{p},\omega_n)=T_c\sum_{i,j}\sum_{\mathbf{k}\nu_n}\sum_{\gamma,\gamma',\delta,\delta'} g^i_{\alpha\gamma}(\mathbf{p},\mathbf{k})\tilde{V}^{ij}_{S,T}(\mathbf{p}-\mathbf{k},\omega_n-\nu_n)g^j_{\delta\beta}(-\mathbf{k},-\mathbf{p})G_{\gamma\gamma'}(\mathbf{k},\nu_n)G_{\delta\delta'}(-\mathbf{k},\nu_n)\phi_{\gamma'\delta'}(\mathbf{k},\nu_n) , \quad (7)$$

where ω_n,ν_n are fermion Matsubara frequencies. The subscripts S,T refer to singlet and triplet channel, respectively, and $V_S=\Gamma_\rho-3\Gamma_\sigma$, $V_T=\Gamma_\rho+\Gamma_\sigma$. Equation (7) has the same form as the equation for the effective interactions [Eq. (3)]; we solve for T_c using a procedure similar to Eq. (5) (see Appendix for details), writing Eq. (7) (in an obvious notation) as

$$[1-\tilde{V}\Pi]\phi=\mu\phi , \quad (8)$$

with T_c determined by $\mu(T_c)=0$. The pairing amplitude will be sizable only in the conduction band, and to allow for superconducting states of different symmetry we write

$$\phi_{\alpha\beta}(p)=u_\alpha(p)u_\beta(p)\sum_i a^i h^i(\mathbf{p}) , \quad (9)$$

where $u_\alpha(p)$ is the conduction-band wave function, and $h^i(\mathbf{p})$ are mutually orthogonal basis functions. In the singlet channel, we have made the following choice:

$$\begin{aligned} h^1(\mathbf{p})&=1 ,\\ h^2(\mathbf{p})&=\cos k_x+\cos k_y ,\\ h^3(\mathbf{p})&=2\cos k_x\cos k_y ,\\ h^4(\mathbf{p})&=\cos k_x-\cos k_y ,\\ h^5(\mathbf{p})&=2\sin k_x\sin k_y . \end{aligned} \quad (10)$$

The functions h^{1-3} have A_{1g} (extended s-wave) symmetry, h^4 is of B_{1g} ($d_{x^2-y^2}$), and h^5 is of B_{2g} (d_{xy}) symmetry. These functions allow for up to second-neighbor correlations in real space. We have not found any regime of attraction in the triplet channel, which will not be discussed further. In the present paper, we shall solve Eq. (7) within the BCS approximation of taking the interactions frequency independent up to a cutoff (either the band-width or the characteristic excitation energy, whichever is lower). Calculations including the full dynamics of the collective mode will be published elsewhere.[32]

III. RESULTS

A. Collective modes

We first present results within the Hartree-Fock approximation for the propagators. As we remarked above, zeros of the operator $\chi_{\rho,\sigma}$ yield the dispersion relation for collective modes. In Fig. 3 we show Reλ along the Reω axis for both charge and spin channels for $\mathbf{q}=(0,0)$, and $\mathbf{q}=(\pi,\pi)$. The zero crossings of Re$\lambda(\mathbf{0},\omega_0)$ mark collective charge excitations (excitons); in the present approximation, these modes are undamped (Im$\lambda=0$) provided that they lie outside the continuum of particle-hole excitations. We see that the lowest eigenvalue crosses zero at an energy $\sim 2t$ in the charge channel and $\sim 3.5t$ in the spin channel. These crossings mark the position of singlet or triplet A_{1g} excitons, the latter being damped (Im$\lambda\neq 0$) because it lies in the continuum, while the former has moved down just below the band edge. In earlier calculations[3] we presented results with $t'=0$; in that case, additional E_u and B_{1g} excitons were also found. With $t'=0$, the nonbonding band is completely flat, and excitons formed from a hole in this band and an electron at E_F are bound for arbitrarily small V; this binding is weak and easily destroyed by a small mass for the hole as occurs for nonzero t'.

There are no propagating modes at large momentum, where the excitations are dominated by the intraband particle-hole excitations. In the spin channel, the lowest eigenvalue is small at low energies, signifying the proximity to a SDW phase.

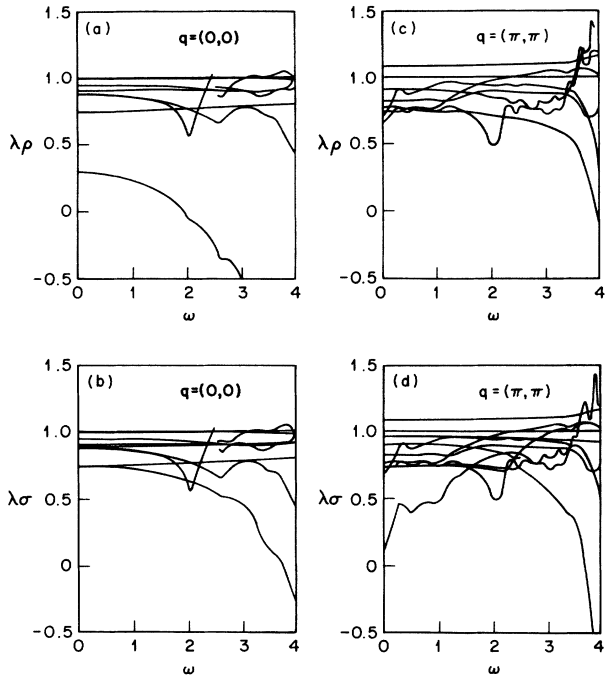

FIG. 3. Real part of the eigenvalues of the non-local charge [(a) and (c)] and spin [(b) and (d)] susceptibilities $\lambda_{\rho,\sigma}(\mathbf{q},\omega)$ from the solution of Eq. (4). Parameters are $U=1.5$, $V=1.5$, $U_p=0$, $\epsilon=0$, $t'=0.5$. (a) and (b), $\mathbf{q}=(0,0)$; (c) and (d), $\mathbf{q}=(\pi,\pi)$.

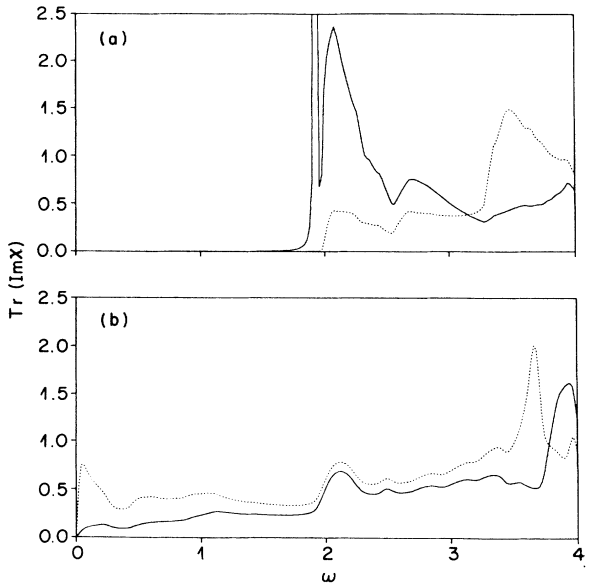

FIG. 4. Spectral function Tr Imχ for the same parameters as Fig. 3. The sharp excitonic features in the charge channel at $q=0$ have been broadened by adding a small imaginary part to the frequency $\mathrm{Im}\omega=10^{-3}$. Solid lines, χ_ρ; dashed lines, χ_σ; (a) $\mathbf{q}=(0,0)$; (b) $\mathbf{q}=(\pi,\pi)$.

In Fig. 4 we show the spectral function Tr Im$\chi_{\rho,\sigma}$ for the same parameters as Fig. 3. At $\mathbf{q}=\mathbf{0}$, there is a gap in the particle-hole spectrum (from nonbonding to antibonding states), and the A_{1g} singlet exciton is s sharp feature (actually a δ function, broadened in the figure by calculations performed at $\mathrm{Im}\omega=10^{-3}$). The triplet exciton is visible as a broad resonance. At momenta q, near the zone boundary, there is a large enhancement of the spin susceptibility over the charge susceptibility at low energies. This feature comes from the soft "paramagnons" seen already in Fig. 3(d).

For the case of charge fluctuations at $\mathbf{q}=(0,0)$, we have separated the spectrum into components of different symmetry (see the Appendix). Figure 5(a) shows the results for the same parameters as Fig. 4. Only the E_u components are optically active, and the solid curve is proportional to the optical absorption $\mathrm{Im}[\epsilon^{-1}(\mathbf{0},\mathbf{0},\omega)]^{-1}$ [$\epsilon(\mathbf{G},\mathbf{G}',\omega)$ is the nonlocal dielectric matrix at reciprocal lattice vectors $\mathbf{G},\mathbf{G}'$]. We also show here some typical results for different parameter values. In Fig. 5(b) [the same parameters as Fig. 5(a), except that here $t'=0$] we find excitons in all symmetries. The position of the A_{1g} mode close to the optical edge in Fig. 5(a) is an accident of parameters; in Fig. 5(c) we show the spectrum at smaller values of U and V, where the mode now lies in the continuum as it does also in Fig. 5(b) (however, in the special case of $\epsilon,t'=0$, the A_{1g} mode is undamped because there are no nonbonding-antibonding transitions of A_{1g} symmetry).

The "excitonic" charge-transfer mode is not strongly $\mathbf{q}$ dependent, although it becomes damped when within the continuum of particle-hole excitations. In Fig. 6 we plot the dispersion along $\mathbf{q}=(\zeta,\zeta)$ and $\mathbf{q}=(\zeta,0)$, with the continuum of excitations hatched. We remark that there exist decay channels for the charge-transfer mode which have not been included in the time-dependent Hartree-Fock calculations of Figs. 3–6; both decay into two particle-hole pairs, as well as a finite lifetime for the single-particle propagators will lead to a nonzero lifetime, as shown earlier.[3]

In this picture, instabilities of the metallic state will be signified by the softening of a collective mode: namely $\lambda(\mathbf{q},\omega=0)\Longrightarrow 0$. In Fig. 7 we identify the three instabilities that we find: a SDW or CDW with $\mathbf{q}$ near (π,π), and a $\mathbf{q}=(0,0)$ A_{1g}-symmetry charge-transfer mode. We note that the position of the CDW and SDW instabilities is sensitive to the band-structure parameters ϵ,t,t', because of their influence on the nesting properties of the Fermi surface. In contrast, the CTI is much less sensitive, because the oscillator strength for the CTR is derived from high-energy electronic transitions. However, to this order in the calculation, we always find that the CTI is preempted by a CDW transition. This is not true when self-energy corrections are included in the propagators before the solution of Eq. (3), where for large doping the CTI becomes the dominant instability, and both the SDW and CDW are suppressed. These effects are also shown in Fig. 7 where we have included second-order self-energy corrections (open symbols).[3]

B. Single-particle spectra

The collective modes, both of spin and charge, may heavily renormalize the single-particle spectra, particu-

larly in the vicinity of phase boundaries where the collective modes are soft. These effects can be studied by calculating the self-energy [Eq. (6)] and evaluating the single-particle spectral function $A(k)=\mathrm{Tr}\,\mathrm{Im}[\omega-E(\mathbf{k})-\Sigma(k)]$, where $k=(\mathbf{k},\omega)$. In the absence of self-energy corrections, $A(k)$ will be a sum of δ functions at the positions of the single-particle bands. We have found that self-energy is not strongly momentum dependent and can be regarded as a renormalization of the parameters ϵ,t,t', which is approximately a function of frequency alone.[3]

Some representative spectra are shown for the Hubbard model ($U_p=V=0$) in Fig. 8. We have chosen E_f as the zero of energy, so that the bands are shifted down, by $\sim 2t$, from the band structure specified by Eq. (1). Several features are apparent. The quasiparticles acquire a finite lifetime away from the Fermi surface, although the bands are still clearly defined; the peaks have a finite width. There is also considerable narrowing of the conduction band and also the development of a finite gap (at $k=0$) between bonding and antibonding states, where none existed before (this calculation was performed with $\epsilon=0$, and the $k=0$ splitting is between O and Cu orbitals).

In Fig. 9 we show the integrated density of states projected onto both Cu and O orbitals, comparing the unrenormalized band structure with that for $U=4$. For $U=0$, the band structure yields a sharp peak from the nonbonding O band at $-2t$, and two hybridized bands between Cu and O. For large U, the oxygen local density of states (DOS) is not very much changed, while the Cu local DOS is strongly renormalized. At low energies, the Cu states are mostly incoherent, whereas close to the Fer-

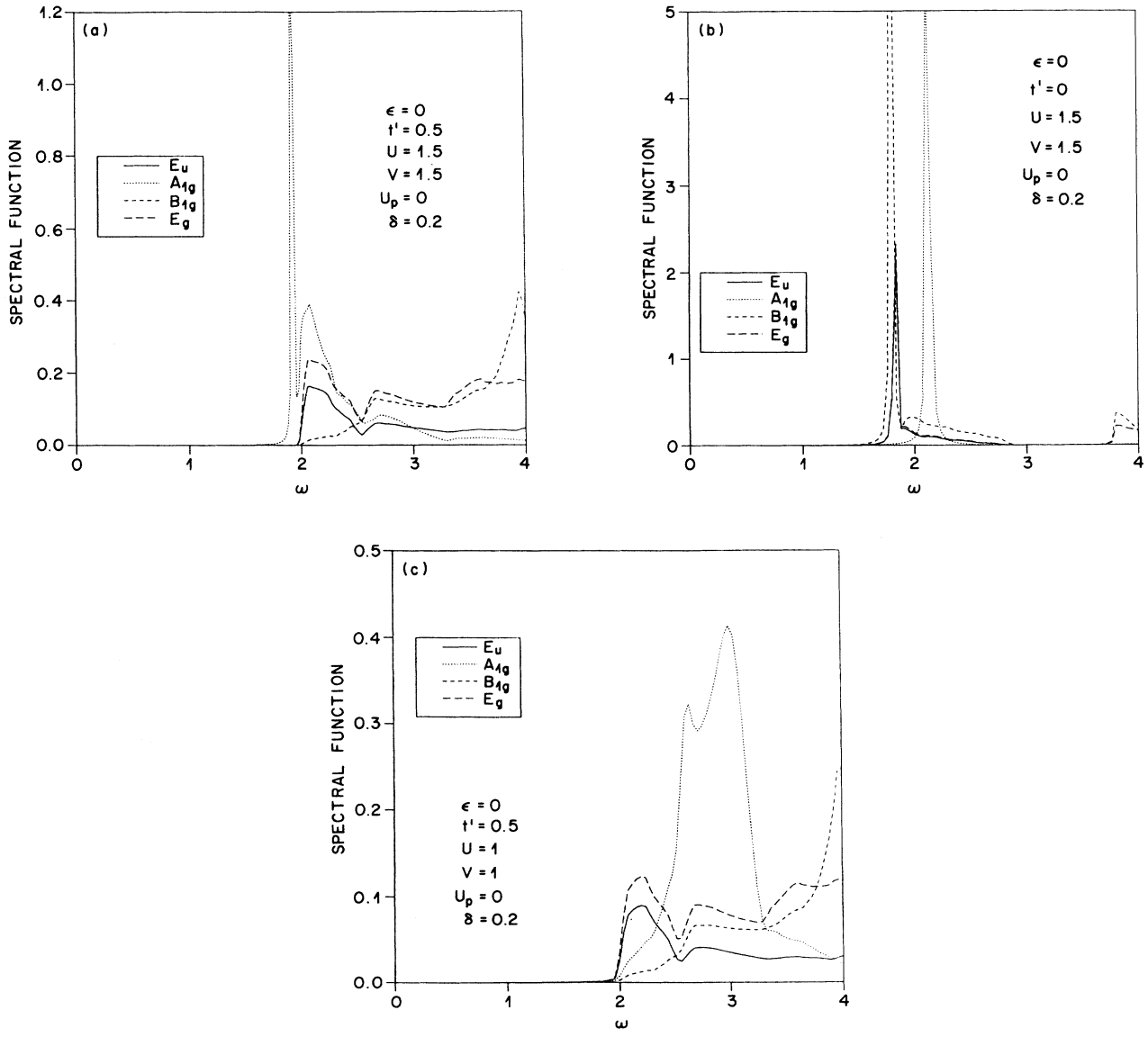

FIG. 5. Spectral function for charge excitations at $\mathbf{q}=(0,0)$ separated into symmetry components, for different values of the parameters.

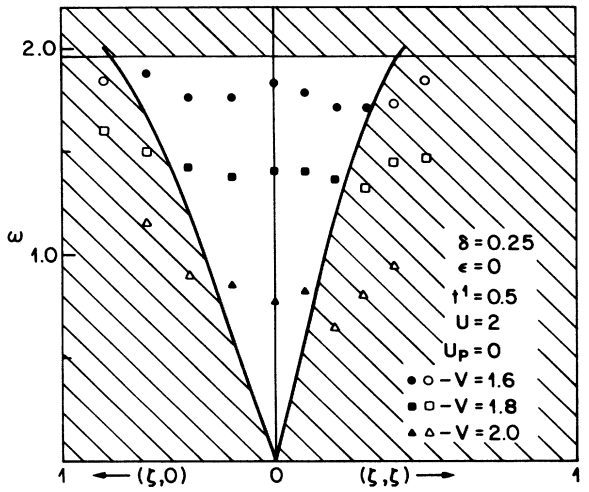

FIG. 6. Dispersion relation for the charge-fluctuation collective modes for three different values of V; hatched areas mark the continuum of particle-hole excitations; solid symbols represent undamped excitations (outside the particle-hole continuum); modes which remain underdamped in the continuum are shown by open symbols.

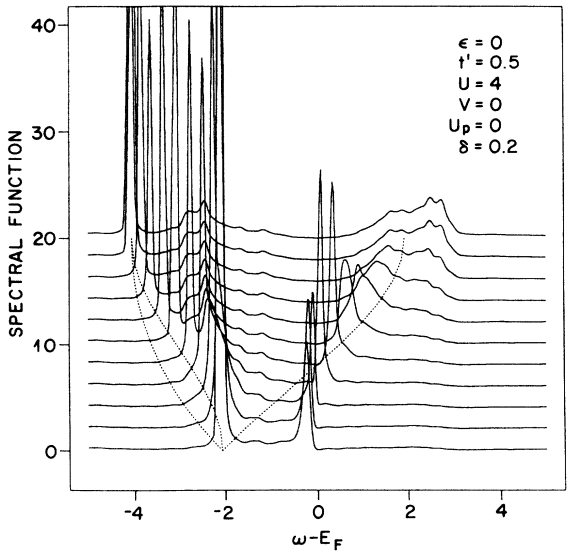

FIG. 8. Electron spectral function as a function of energy at fixed momenta along $\mathbf{k}=(\zeta,\zeta)$. The dotted line shows the dispersion relation for the single-particle Hamiltonian. Energies are measured relative to the Fermi energy.

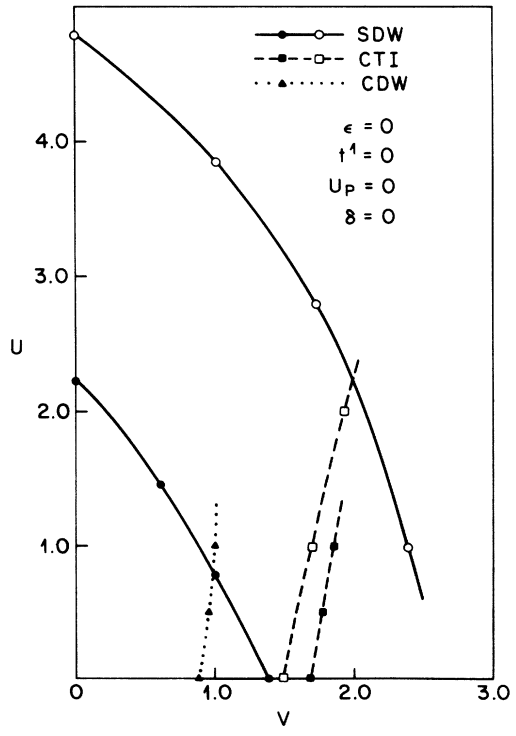

FIG. 7. Phase diagram as a function of U, V at a doping $\delta=0.2$. In all cases, we mark the instabilities of the metallic phase, even though some of the phases may not be accessible on account of preemption by other transitions. Solid (open) symbols are the results without (with) second-order self-energy corrections.

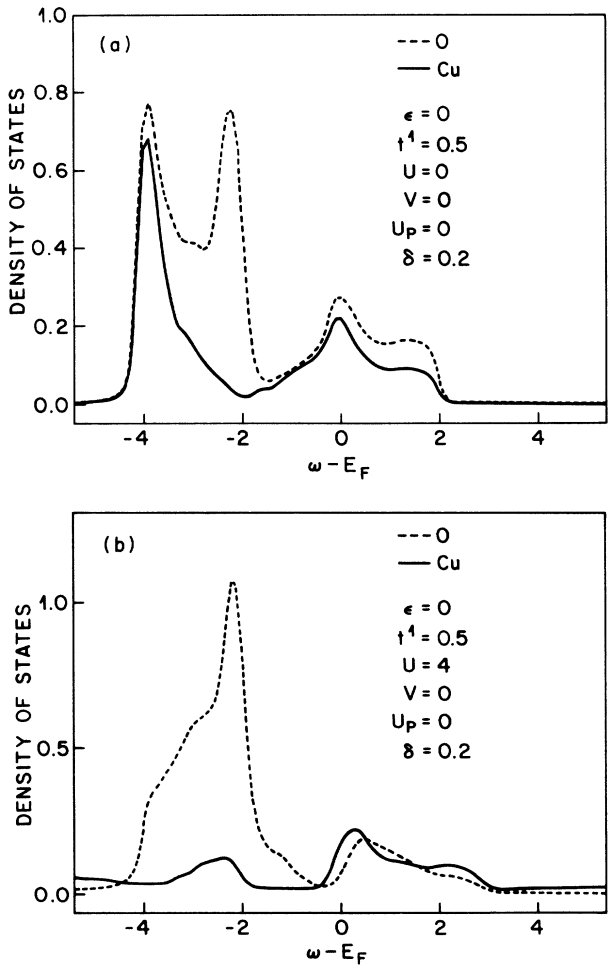

FIG. 9. Integrated density of states on Cu (solid line) and O (dashed line) for $\delta=0.2$, $\epsilon=0$, $t'=0$, and $V=U_p=0$: (a) $U=0$; (b) $U=4$.

mi surface the band narrowing visible in Fig. 8 increases the Cu character relative to O. At energies ~ 2, there is an extra peak not seen in the bare DOS; this feature is the analog of the "upper Hubbard band" in a strong-coupling ($U \to \infty$) picture, and it occurs at an energy of roughly $E_d + U$, as expected.

We also study the low-energy behavior in the vicinity of the SDW transition. By analogy with the case of electron-phonon interactions,[33] a soft mode would be expected to lead to a large effective-mass enhancement and considerable rearrangement of the oscillator strength in the vicinity of E_F. In Fig. 10 we display the low-energy spin-fluctuation spectra at the zone corner (the antiferromagnetic Bragg "peak-to-be") as a function of U, and also as a function of momentum in the (1,1) direction for $U=4$. The SDW here occurs above $U_{\text{crit}}=4.15$, and the very rapid development of spin fluctuations at low energy and large momentum is seen on the approach to the transition. The softening occurs only over a narrow range of $\mathbf{q}$, and the peak position in Fig. 10(b) marks the position of overdamped "paramagnons," which will become the antiferromagnetic spin waves in the ordered SDW state. Because the q dependence is so strong, the softening of the spin fluctuations has only a small effect on the effective mass. In Fig. 11(a) we show the energy dependence of $\mathrm{Im}\Sigma(\omega)$ for the same parameters as Fig. 10(a), and in Fig. 11(b) the calculated effective mass m^*/m. A careful analysis shows that the effective mass should diverge logarithmically at the transition within the present approximation, as in the case of ferromagnetic spin fluctuations considered some time ago.[30] Because we have neglected the weak momentum dependence of Σ,

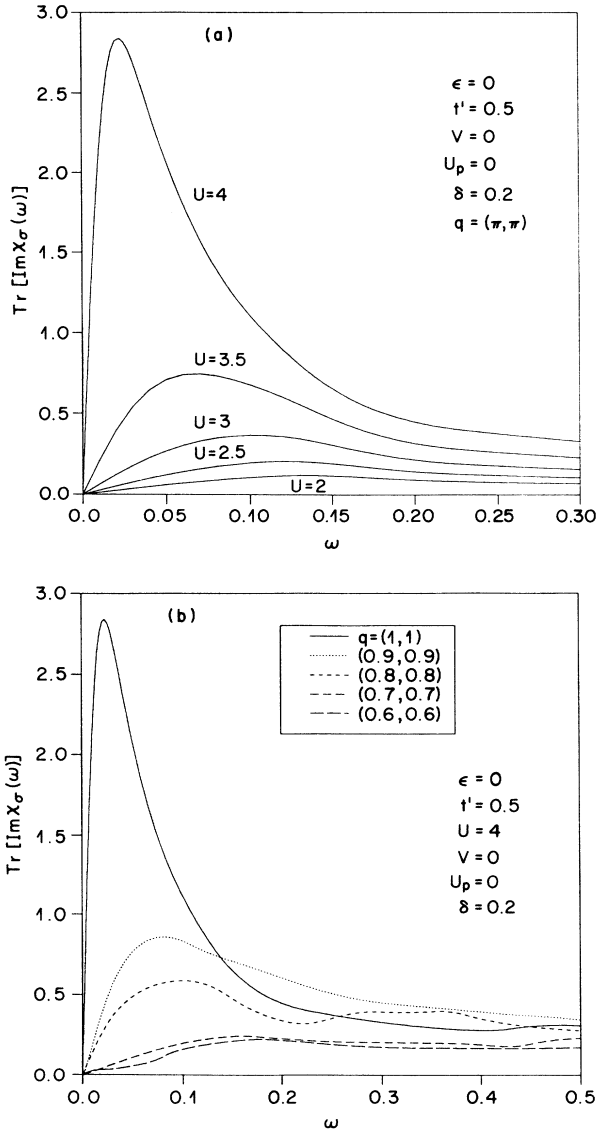

FIG. 10. Spin susceptibility $\mathrm{Tr}\,\mathrm{Im}\chi_\sigma(\mathbf{q},\omega)$: (a) for $\mathbf{q}=(1,1)$ as a function of U; (b) for $U=4$ as a function of $\mathbf{q}=(\zeta\zeta)$. The SDW instability sets in at $U=4.15$ for these parameters.

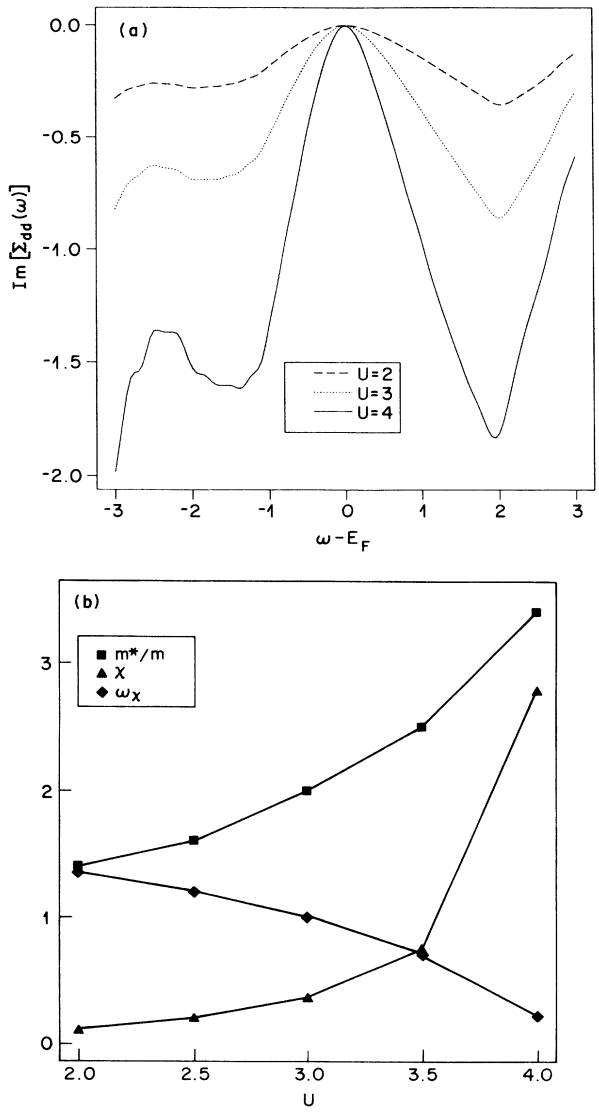

FIG. 11. (a) $\mathrm{Im}\Sigma_{dd}(\omega)$ for the same parameters as Fig. 10(a); (b) effective mass renormalization on the Fermi surface (squares); peak value of the susceptibility (triangles); and frequency ($\times 10$) of the susceptibility peak (diamonds).

the quasiparticle spectral weight $Z(\omega)=[1-\partial\Sigma/\partial\omega]^{-1}$ and the effective mass m^* are inversely related.

C. Superconductivity

Any or all of the low-energy particle-hole fluctuations may be used as mediating bosons for superconductivity. It is convenient to consider the effect of *intra*band and *inter*band fluctuations separately. The former includes the low-energy spin and charge fluctuations, which would yield either the SDW or CDW instabilities; the latter consists of the charge-transfer resonances, principally the mode of A_{1g} symmetry. Calculated phase diagrams (as functions of U, V) are shown in Figs. 12–14 for three different parameter sets; they are all similar in structure. For each set of parameters, we have calculated the effective interaction $\tilde{V}$ both with and without inclusion of the intraband terms in the polarizability P [Eq. (3) and Fig. 1(c)]. Thus we distinguish the effects of the intraband and interband fluctuations on the superconductive pairing. In these figures we show instabilities from the normal state, when $T_c=10^{-4}$; in fact, T_c is positive over almost all of the metallic part of the phase diagram, but usually extremely small.

The effect of the intraband spin fluctuations is to promote B_{1g}-symmetry ($d_{x^2-y^2}$) pairing, as has been found elsewhere.[34] Such d-wave pairing is expected naturally in a model with repulsive interactions and a nearby instability at large momentum. There is also an instability to A_{1g} pairing, which is, in this case, "extended" s wave,

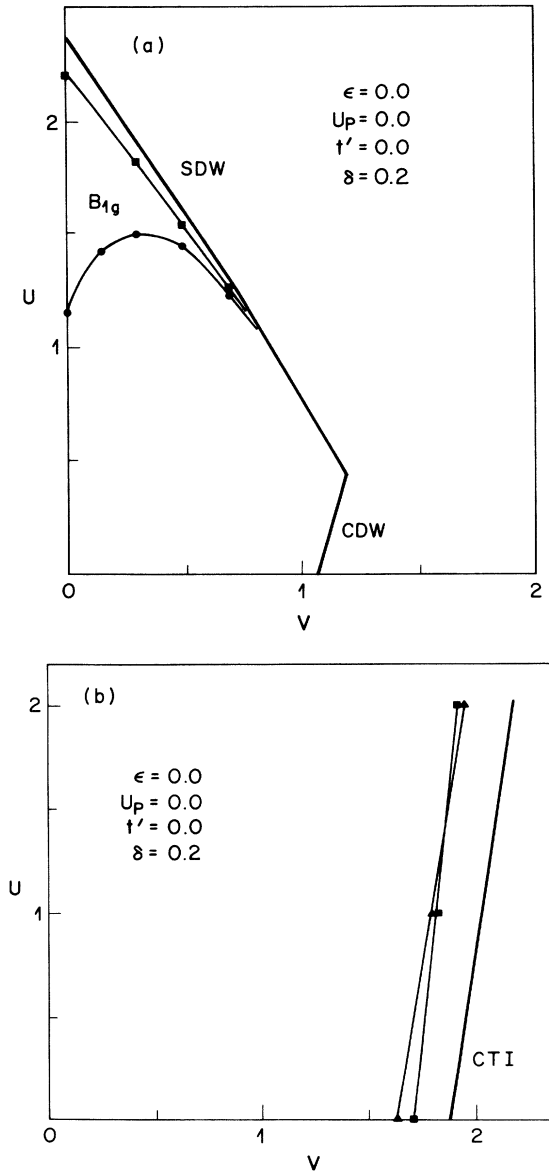

FIG. 12. Instabilities of the normal state for $\epsilon=0$, $t'=0$, and $U_p=0$ with (a) or without (b) the inclusion of intraband coupling terms in the evaluation of the effective interaction. Superconducting instabilities are shown for $T_c=10^{-4}$, in three different symmetries: Circles, B_{1g} ($d_{x^2-y^2}$); squares, A_{1g} (s); triangles, B_{2g} (d_{xy}).

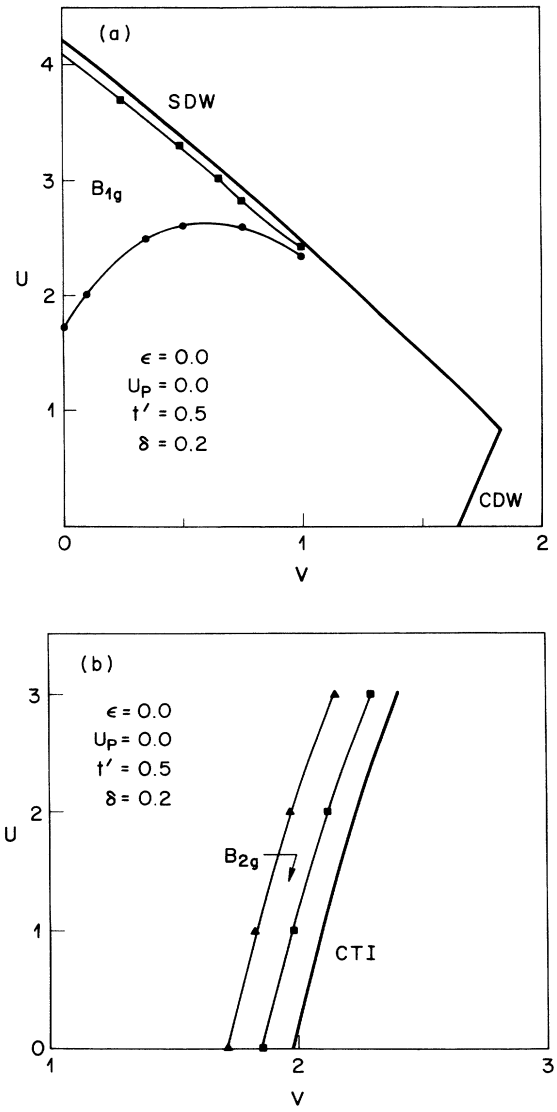

FIG. 13. Same as for Fig. 12, but with $\epsilon=0$, $t'=0.5$, and $U_p=0$.

with eigenvector h^2 [Eq. (10)], although, in all cases, this has a lower transition temperature than for d-wave pairing. Inclusion of O-O hopping ($t' \neq 0$) suppresses the SDW to higher values of U, as shown earlier; but aside from a change in scale for the vertical axis in Fig. 13(a), the pairing is not affected. In contrast, adding a nonzero O-O repulsion U_p [Fig. 14(d)] does not affect the position of the SDW instability (the matrix elements for coupling at the zone boundary do not introduce O-orbital weight), whereas the transition temperature for d-wave pairing is reduced.

The proximity to a CDW instability does not induce a wide region of superconductivity, unlike the case of the SDW. We find a very weak tendency for B_{2g} (d_{xy}) pairing in the vicinity of the CDW transition; but in most cases it is too narrow to be visible on the figure. In contrast, the CTR is more effective in promoting pairing, both of A_{1g} and B_{2g} symmetry, but still the range of superconductivity is narrow in comparison to that from spin fluctuations. We shall explore the reasons for this more deeply later; however, the central reason for the ineffectiveness of charge fluctuations is that they promote *attractive* on-site interactions at the expense of enhancing *repulsive* intersite interactions. The effect of *intra*band fluctuations is further vitiated by the small range of momentum over which the particle-hole interactions are soft, leading to a negligible T_c in the cases we have studied.

The CTI and its associated superconducting states are not accessible in the present calculations on account of the presence of the CDW instability. We showed earlier[3,4] that the inclusion of self-energy corrections suppresses the CDW in favor of the CTI (Fig. 7); nevertheless, the superconducting states persist in the vicinity of the CTI, with a similar phase diagram to that of Figs. 12–14. As the physics of the CTR-induced pairing states is not changed by the inclusion of self-energy corrections, we shall study the pairing mechanism by the simple expedient of neglecting all intraband contributions to the effective interaction, as in Figs. 12(b), 13(b), and 14(b).

In Fig. 15 we show the doping dependence of T_c along with the frequency of the A_{1g} mode; both "extended s" and d_{xy} pairing are favored. For all parameters we have studied, these states are competitive in energy. For the same parameters, in Fig. 16 we show the effective interactions in real space for the singlet channel. They may be interpreted as renormalized values of the bare interactions U, V, U_p: $\Gamma_{dd} = U_{\text{eff}}$, $\Gamma_{pp} = (U_p)_{\text{eff}}$, $\Gamma_{pd} = V_{\text{eff}}$, and Γ_{xy} the effective interaction between nearest-neighbor oxygen carriers, which was not included in Eq. (1). We see that the CTR promotes attraction in three of the channels, whereas the Cu-O interaction becomes large and repulsive close to the transition. The magnitude of the individual interactions is quite large, and it is the competition between the repulsive and attractive parts that

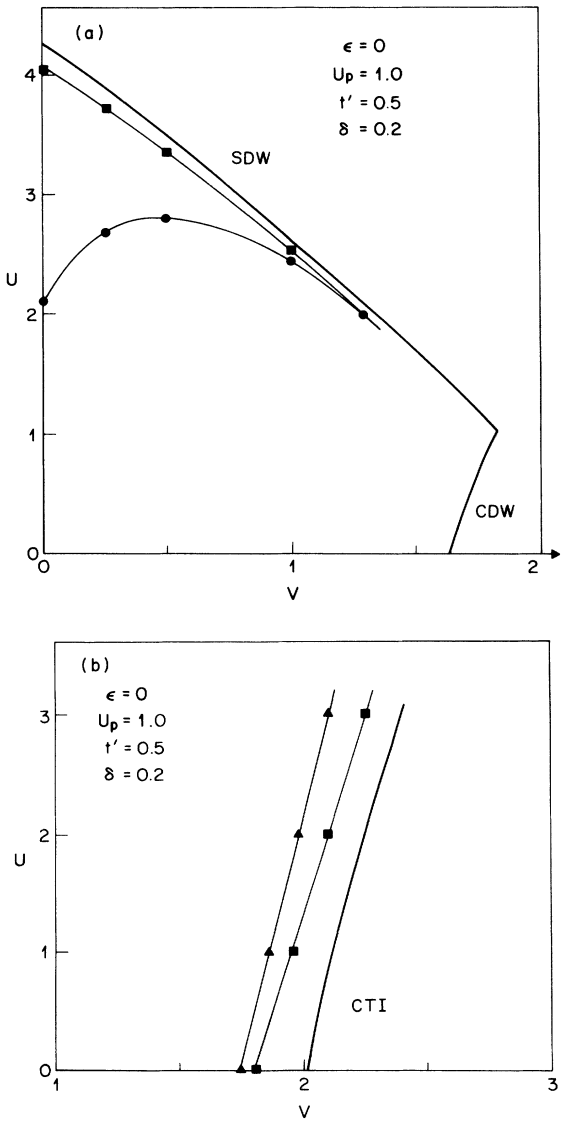

FIG. 14. Same as for Fig. 12, but with $\epsilon = 0$, $t' = 0.5$, and $U_p = 1$.

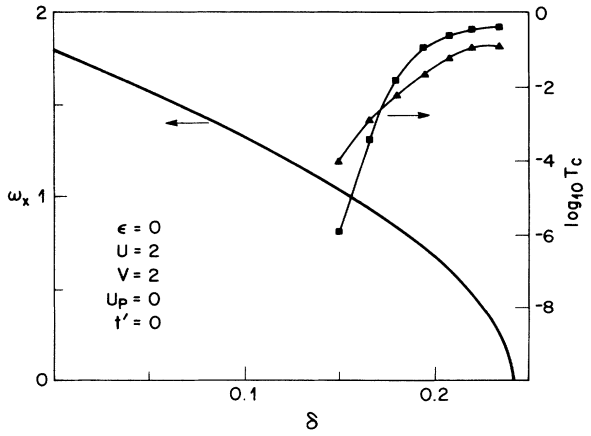

FIG. 15. A_{1g} ($\mathbf{q}=\mathbf{0}$) mode frequency (left scale) and superconducting transition temperatures (right scale: squares, A_{1g}; triangles, B_{2g}) as a function of doping, for the parameter values shown.

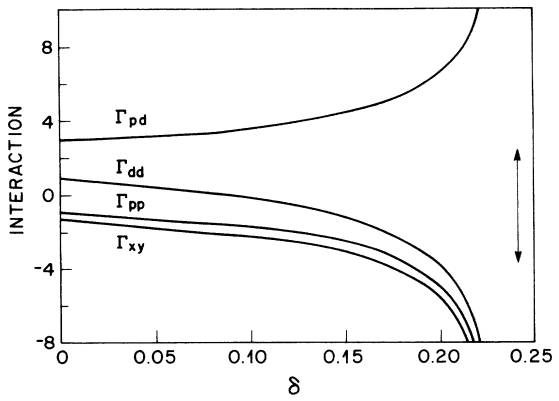

FIG. 16. Effective interactions between particles on near-neighbor sites as a function of doping, for the same parameters as Fig. 15. The arrow marks the CTI.

accounts for the low T_c over most of the range of doping in Fig. 15.

The origin of this behavior is easily seen by a simple argument. We assume an incoming particle on a Cu atom, which will then excite an A_{1g}-symmetry CTR; thus charge will be locally depleted from the Cu site and pushed symmetrically onto the O neighbors. A second particle of the same charge will then experience extra *attraction* to the Cu site ($\Gamma_{dd}<0$) but increased *repulsion* from the O site ($\Gamma_{pd}>0$). This argument can be rerun with the initial particle on the O site and will yield $\Gamma_{pp}<0$, and $\Gamma_{xy}<0$, with the latter on account of the excited mode having the full symmetry of the square lattice. The sign of the various interactions accounts for the symmetry of the pairing in a natural way, and, in particular, we find that the eigenvector for A_{1g} pairing is about (0.1, 0.9, 0.1) on the basis (h^1, h^2, h^3) of Eq. (10). The real-space node in h^2 at the origin suppresses the copper character in the pair wave function. Note that the reason for the extended s character is here different from that in the case of the simple Hubbard model; here, the nearest-neighbor Cu-O repulsion is avoided, whereas, in the pure Hubbard model, it is the on-site repulsion that is the culprit.

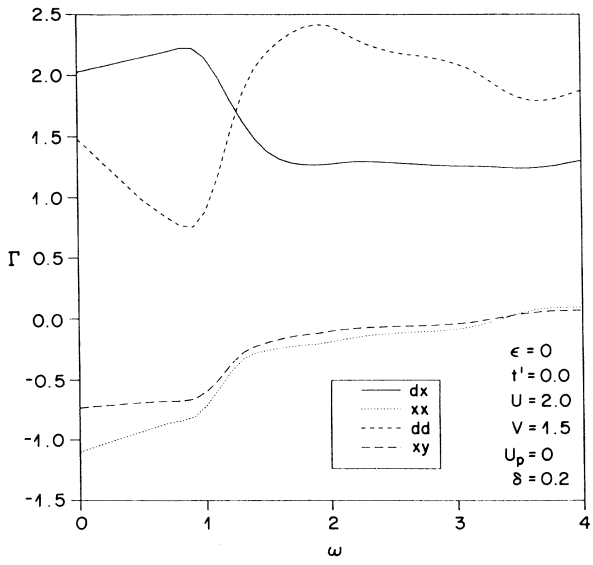

FIG. 17. Frequency dependence of the effective particle-particle interactions.

In Fig. 17, we show the frequency-dependent interactions near the charge-transfer instability. Here, we have included self-energy corrections to the second order in the propagators, but the effect of the A_{1g} mode is clearly visible, with a characteristic frequency $\sim t$, in this case. The interactions do not have a strong frequency dependence, so that our use of the BCS approximation appears justified.

IV. DISCUSSION

The approximations we have used have a number of deficiencies, which are certainly serious quantitatively but may leave the qualitative description of the metallic state valid. Principally, the Hartree-Fock approximation gives a poor description of the large-U Hubbard model, because the on-site correlations can only be included by introducing long-range antiferromagnetic order. Thus the tendency to SDW (and also CDW) formation is overestimated. This defect is partially cured by the inclusion of self-energy corrections; in Sec. III B we showed the development of a finite lifetime for quasiparticles (away from E_F), as well as effective-mass corrections, and the beginnings of the development of separate "bands" for singly and doubly occupied states. Earlier,[3] it was shown that both the CDW and SDW instabilities were shifted to larger values of the interaction parameters. Close to the SDW transition, the carriers are electrons, albeit with an increased effective mass; this is an inescapable consequence of a Fermi-liquid ground state.

Whether or not the metallic (nonsuperconducting) state of the high-T_c cuprates is a Fermi liquid is a matter still not settled, although photoemission experiments at 100 K show a sharp Fermi surface with a resolution of 20 meV.[35] It has been suggested[36] that many of the unusual normal-state properties can be reconciled within an "almost Fermi-liquid" picture, where the Fermi surface is sharply defined at zero temperature, but the quasiparticle lifetime vanishes linearly with energy about E_F (rather than quadratically, as in a Fermi liquid). Such behavior is not produced by the calculations in this paper, but may arise naturally in two-dimensional models with attractive interactions in the s-wave channel.[37] If this is the case, there is no reason to expect that the behavior at moderate energies (i.e., $\gtrsim T_c$) will differ significantly from that presented here.

Our results for the Hubbard model ($V=U_p=0$) are very similar to those for the single-band model,[13,34] with a broad region of d-wave superconductivity on the metallic side of the SDW boundary. This single-band behavior occurs despite the strong hybridization between Cu and O states,[38] although we find, of course, that the SDW instability is suppressed by changes in the band structure to reduce the Cu occupancy near E_F. The pairing is

suppressed by nonzero interatomic interactions V.

In contrast, we find that intraband charge fluctuations (near a CDW phase) are not at all effective for inducing superconductivity. That others[26,27] have found them more favorable may arise from at least two causes, but probably not from the differences in the microscopic models. First, we argued above that to evaluate an effective interaction parameter by a Fermi-surface average (as is usual in the case of phonons) is inappropriate when the characteristic energy of the fluctuating modes is comparable to the bandwidth of the carriers. In particular, for a uniform s-wave state [eigenvector h^1 in Eq. (10)], the kernel of the gap equation is the effective interaction averaged over all momenta (weighted by the wave functions); this we find to be invariably repulsive, even though there is a small region of attraction resulting from particle-hole momentum transfers near $2k_F$. Second, we have also found that the local-field corrections produce non-negligible effects, and we have made no approximations[27] to the exchange interaction.

We do find that extended s-wave (A_{1g} symmetry) and d_{xy} pairing are favored by the existence of a low-energy charge-transfer resonance, which will occur close to a valence instability of the crystal. Our results appear to be in general agreement with those of Wagner *et al.*,[24] in particular, as to the identification of three instabilities (SDW, CDW, and CTI) and their enhancement of superconductive pairing. They found that a finite value of V favors s-wave pairing, and also (weakly) $d_{x^2-y^2}$, but had always a small repulsion for d_{xy}, except in the case where U_d is also large. The reasons for the differences from our results are not clear, but may arise because these authors calculate a Fermi-surface averaged coupling constant, which we argued above was inaccurate in the case of virtual excitations of high energy. The symmetry of the pairs is strongly influenced by the details of the band structure, and especially by the relative Cu and O weights.

It is important to stress that the physics involved in the CTR-mediated pairing is different from that arising within "conventional" exciton or plasmon mechanisms, which rely on the long-range part of the Coulomb interaction, and which were discussed briefly in the introduction. For a number of reasons,[7-9] such mechanisms do not give rise to high transition temperatures. If one neglects local-field corrections, the effective interaction between quasiparticles can be written in terms of a single dielectric function $\epsilon(q,\omega)$; for a single collective mode, this can be given the model form[9] of

$$\epsilon(q,\omega)=1-\frac{\Omega_q^2}{\omega^2-\omega_q^2} . \tag{11}$$

For example, for a plasmon in the random-phase approximation (RPA) $\Omega_q=\omega_p$, $\omega_q=\omega_p q/q_0$ with $q_0^2=(4/\pi)e^2mk_F$. A similar formula will apply for a transverse exciton, but with $\omega_q=\omega_0$, the exciton frequency at small momenta, as in the model of Allender, Bray, and Bardeen,[5,32] for example. It is clear that the static interaction is invariably repulsive (except at $q=0$, in the case that $\omega_0=0$); with an exciton, the interaction is repulsive up to the exciton frequency ω_q. The effective interaction $v(q)/\epsilon(q,\omega)$ is always repulsive below the exciton frequency and is attractive in the range $\omega_q<\omega<(\Omega_q^2+\omega_q^2)^{1/2}$; inasmuch as attraction at low energies is expected to be favorable for superconductivity, it would seem that *dipole-active* modes are to be avoided (assuming that the coupling to quasiparticles is, in fact, Coulombic).

The attraction from plasmons was considered in detail by Rietschel and Sham, and Grabowski and Sham,[9] who found that a simple RPA calculation yielded a large T_c, reduced to the range of tens of kelvins by self-energy corrections (at a large $r_s\sim 5$).[39] Inclusion of leading-order vertex corrections led to a suppression of superconductivity by processes violating Migdal's theorem when $\omega_p/E_F\gtrsim 0.1$.[9] Part of the reason for the ineffectiveness of plasmons is, as mentioned above, that the static interaction is invariably repulsive; even without the deleterious vertex corrections, it was found that $T_c/E_F\lesssim 10^{-3}$. The transition temperature is thus determined as much by the frequency structure of the interaction as by its magnitude.

The major reason for the poor success of the early excitonic mechanisms is the failure to include umklapp processes (local-field corrections) in a consistent fashion. In the conventional BCS phonon mechanism, coupling to transverse phonon modes is induced via umklapps, despite the appearance of the transverse phonon modes as a *pole* in the dielectric function [as in Eq. (11)].[40] While these difficulties were appreciated at the time,[8,32] their resolution requires a detailed calculation. With a more general formulation of the problem including local-field corrections, it is possible to have *static attraction* at short distances. The general stability condition within RPA is that all eigenvalues $\lambda(\mathbf{q},\omega=0)$ [Eq. (5)] of the dielectric matrix must be positive at zero frequency; this is a sufficient condition to ensure that the long-wavelength dielectric constant is also positive. However, it allows for static attraction in some but not all channels. If the interaction does not have a net attractive component, the superconductivity is then more robust, and dynamical corrections are not expected to play such an important role. For a more general formulation of the dielectric response, even the positivity constraint on the test-charge dielectric function is relaxed,[41] so that the repulsion can, in principle, be further reduced.

The effects of self-energy corrections are, however, quite large. While the superconducting kernel is the result of a detailed balance between repulsive and attractive terms (and is therefore small) interactions of both signs give additive corrections to the self-energy; we found earlier a reduction of T_c by typically an order of magnitude from self-energy effects.[4] This is similar in magnitude to the reductions obtained for the plasmon problem.[9]

There is no reason to believe that large values of U have much effect on the CTR, although, within our calculations, the CTR is pushed to high energies as U increases. This is the same defect in the model discussed above; a large U suppresses *all* charge fluctuations within

the HF picture, whereas, realistically, only double occupancy is suppressed. Gutzwiller calculations in the large-U limit indeed show that the CTI persists[2] and also indicate that a superconducting ground state of extended s-wave symmetry is favored nearby.[42] Monte Carlo calculations[20] have also shown that a large enhancement of the charge-transfer fluctuations can be induced by V, but did not explore the region $V \sim t$ for pairing.[43]

We have neglected the dynamics of the interactions in the present calculations, using the BCS approximation. We believe that this is justified, because the characteristic mode energy is generally comparable in magnitude to the conduction bandwidth. Recent calculations using a model for the CTR, but including the full dynamics within the Eliashberg equations, support this.[32] However, the numerical values of the calculated T_c, for this and other reasons, should be regarded as approximate.

If a low-energy CTR mode exists, it will be difficult to identify because it is optically forbidden. However, resonance Raman measurements have indicated the presence of an even symmetry oscillator at an energy ~ 2 eV in the insulating La_2CuO_4.[44] A charge fluctuation mode will couple to phonons of the same symmetry. While there are no A_{1g} phonon modes of a single 2D layer with in-plane vibrations, all of the Cu-O superconductors do have Γ-point A_g modes involving some motion of atoms out of the plane. Frozen phonon calculations of the axial oxygen A_{1g} mode in La_2CuO_4 have shown that this phonon induces charge rearrangements between the planar Cu and O.[45] This quasistatic charge transfer can be regarded as a measure of the low-frequency response of the A_{1g} CTR to an external potential, because the coupling of the O_z motion to the layer is mostly via modulation of the ionic Madelung potential.[45] Experimental evidence for the coupling of A_g-symmetry phonons with charge fluctuations in the plane can also be adduced from the asymmetric Fano line shapes found for several modes in Raman scattering from $YBa_2Cu_3O_7$.[46] Structural changes involving axial O displacements have also been reported[47] near T_c in $YBa_2Cu_3O_7$, and have been suggested to be important in other cuprates as well[48] (although these authors propose a direct role in pairing for this phonon mode, whereas we would regard it as a spectator).

A low-energy CTR would also imply that the crystal would be close to a structural instability, corresponding to a sudden valence change of the Cu and O ions. This transition will be of the first order in nature, because the A_{1g} mode couples to a uniform volume strain. In the complicated environment of realistic materials, it may indeed signify a complete breakup of the structure. The small "buckling" distortions of the plane that are prevalent in these compounds can be understood as the results of a compromise between the "natural" lattice constants of the CuO_2 plane and the sandwich "building blocks."[49] The softening of the CTR might lead to a change in the lattice constant of the CuO_2 plane, which is large enough to render the crystal structurally unstable. It is therefore interesting that it is indeed very difficult to dope these materials beyond some critical concentration while maintaining a homogeneous phase.

ACKNOWLEDGMENTS

This work is an outgrowth of continuing collaboration with E. Abrahams, S. Schmitt-Rink, and C. M. Varma. Many useful discussions with S. N. Coppersmith, P. A. Fleury, K. B. Lyons, A. Millis, J. Orenstein, P. E. Sulewski, and G. A. Thomas are gratefully acknowledged. Correspondence and conversations with M. L. Cohen on the nature and relevance of local-field corrections has been invaluable in the presentation of this work.

APPENDIX

In the Appendix, we provide details of the basis used to solve the particle-hole T matrix. The basis functions $g^i_{\alpha\beta}(\mathbf{k}, \mathbf{k}+\mathbf{q})$ used are as follows:

$$\begin{aligned}
g^1_{\alpha\beta}(\mathbf{p}+\mathbf{q}, \mathbf{p}) &= g^5_{\beta\alpha}(\mathbf{p}, \mathbf{p}+\mathbf{q}) \\
&= \delta_{\alpha d}\delta_{\beta x}\cos(\tfrac{1}{2}ap_x) , \\
g^2_{\alpha\beta}(\mathbf{p}+\mathbf{q}, \mathbf{p}) &= g^6_{\beta\alpha}(\mathbf{p}, \mathbf{p}+\mathbf{q}) \\
&= \delta_{\alpha d}\delta_{\beta x}\sin(\tfrac{1}{2}ap_x) , \\
g^3_{\alpha\beta}(\mathbf{p}+\mathbf{q}, \mathbf{p}) &= g^7_{\beta\alpha}(\mathbf{p}, \mathbf{p}+\mathbf{q}) \\
&= \delta_{\alpha d}\delta_{\beta y}\cos(\tfrac{1}{2}ap_y) , \\
g^4_{\alpha\beta}(\mathbf{p}+\mathbf{q}, \mathbf{p}) &= g^8_{\beta\alpha}(\mathbf{p}, \mathbf{p}+\mathbf{q}) \\
&= \delta_{\alpha d}\delta_{\beta y}\sin(\tfrac{1}{2}ap_y) , \\
g^9_{\alpha\beta}(\mathbf{p}+\mathbf{q}, \mathbf{p}) &= \delta_{\alpha d}\delta_{\beta d} , \\
g^{10}_{\alpha\beta}(\mathbf{p}+\mathbf{q}, \mathbf{p}) &= \delta_{\alpha x}\delta_{\beta x} , \\
g^{11}_{\alpha\beta}(\mathbf{p}+\mathbf{q}, \mathbf{p}) &= \delta_{\alpha y}\delta_{\beta y} .
\end{aligned} \tag{A1}$$

By inspection, this basis may be separated into symmetry components of the lattice at $\mathbf{q}=0$. We then get

$$\begin{aligned}
&A_{1g} \quad g^2+g^4,\ g^6+g^8,\ g^9,\ g^{10}+g^{11} , \\
&B_{1g} \quad g^2-g^4,\ g^6-g^8,\ g^{10}-g^{11} , \\
&E_u \quad g^1+g^5,\ g^3+g^7 , \\
&E_g \quad g^1-g^5,\ g^3-g^7 .
\end{aligned}$$

The direct V_D and exchange V_X interactions [see Eq. (2)] are then given by

$$\begin{aligned}
V^{ij}_X(\mathbf{q}) &= 2V\delta_{ij}(i \le 8) + U\delta_{i9}\delta_{j9} \\
&\quad + U_p(\delta_{i10}\delta_{j10}+\delta_{i11}\delta_{j11}) ,
\end{aligned} \tag{A2}$$

$$\begin{aligned}
V^{ij}_D(\mathbf{q}) &= U\delta_{i9}\delta_{j9} + U_p(\delta_{i10}\delta_{j10}+\delta_{i11}\delta_{j11}) \\
&\quad + 2V\cos(\tfrac{1}{2}aq_x)(\delta_{i9}\delta_{j10}+\delta_{i10}\delta_{j9}) \\
&\quad + 2V\cos(\tfrac{1}{2}aq_y)(\delta_{i9}\delta_{j11}+\delta_{i11}\delta_{j9}) .
\end{aligned} \tag{A3}$$

All elements unspecified in Eqs. (A2) and (A3) are zero.

The vertex in the particle-particle channel [Eq. (7)] is not in the same convenient factorizable form as the particle-hole interaction of Eq. (2). However, we may introduce a new orthogonal basis $\tilde{g}$, so that

$$\sum_{ij} g^{i}_{\alpha\gamma}(\mathbf{p},\mathbf{k}) V^{ij}(p-k) g^{j}_{\delta\beta}(-\mathbf{k},-\mathbf{p}) = \sum_{ij} \tilde{g}^{\,i}_{\alpha\beta}(\mathbf{k},-\mathbf{k}) \tilde{V}^{\,ij} \tilde{g}^{\,j}_{\gamma\delta}(\mathbf{p},-\mathbf{p}) \,. \quad \text{(A4)}$$

Now the integral equation becomes a matrix problem, as in the particle-hole channel. We used a basis set extending the range of interaction to second Cu and first O neighbors in real space [23 components in all, with the first 11 given by (A1)]. Orthogonality of the $\tilde{g}$ allows extraction of the particle-particle interaction $\tilde{V}$ by a single integral over the particle-hole momentum transfer, weighted by products of the $g,\tilde{g}$.

[1] J. G. Bednorz and K. A. Müller, Z. Phys. B **64**, 189 (1986).

[2] S. N. Coppersmith and P. B. Littlewood, Phys. Rev. B **41**, 2646 (1990).

[3] P. B. Littlewood, C. M. Varma, S. Schmitt-Rink, and E. Abrahams, Phys. Rev. B **39**, 12 371 (1989).

[4] P. B. Littlewood, C. M. Varma, and E. Abrahams, Phys. Rev. Lett. **63**, 2602 (1989).

[5] D. Allender, J. Bray, and J. Bardeen, Phys. Rev. B **7**, 1020 (1973); **8**, 4433 (1973).

[6] J. Bardeen, in *Superconductivity in d- and f-Band Metals,* edited by D. H. Douglass (Plenum, New York, 1976), p. 1.

[7] J. C. Inkson and P. W. Anderson, Phys. Rev. B **8**, 4429 (1973).

[8] M. L. Cohen and S. G. Louie, in *Superconductivity in d- and f-Band Metals* (Ref. 6), p. 7.

[9] H. Rietschel and L. J. Sham, Phys. Rev. B **28**, 5100 (1983); M. Grabowski and L. J. Sham, Phys. Rev. B **29**, 6132 (1984).

[10] C. M. Varma, S. Schmitt-Rink, and E. Abrahams, Solid State Commun. **62**, 681 (1987); in *Novel Mechanisms of Superconductivity,* edited by V. Kresin and S. Wolf (Plenum, New York, 1987), p. 355.

[11] E. B. Stechel and D. R. Jennison, Phys. Rev. B **38**, 4632 (1988); A. K. McMahan, R. M. Martin, and S. Satpathy, *ibid.* **38**, 6650 (1988); J. Zaanen, O. Jepsen, O. Gunnarsson, A. T. Paxton, and O. K. Andersen, Physica C (Amsterdam) **153-155**, 1636 (1988); M. S. Hybertsen, M. Schluter, and N. E. Christiansen, Phys. Rev. B **39**, 9028 (1989).

[12] L. F. Mattheiss, Phys. Rev. Lett. **58**, 1028 (1987); J. Yu, A. J. Freeman, and J.-H. Xu, *ibid.* **58**, 1035 (1987).

[13] N. E. Bickers, D. J. Scalapino, and S. R. White, Phys. Rev. Lett. **62**, 961 (1989).

[14] I. E. Dyaloshinskii, Zh. Eksp. Teor. Fiz. **93**, 1487 (1987) [Sov. Phys.—JETP **66**, 848 (1987)]; H. J. Schulz, Europhys. Lett. **4**, 609 (1987); Phys. Rev. B **39**, 2940 (1989).

[15] J. E. Hirsch, Phys. Rev. B **31**, 4403 (1985); J. E. Hirsch and H. Q. Lin, *ibid.* **37**, 5070 (1988); S. R. White, R. L. Sugar, and R. T. Scalettar, *ibid.* **38**, 11 665 (1988); S. R. White, D. J. Scalapino, R. L. Sugar, N. E. Bickers, and R. T. Scalettar, *ibid.* **39**, 839 (1989).

[16] Bickers *et al.* (Ref. 13).

[17] S. N. Coppersmith, Phys. Rev. B **39**, 9671 (1989); and unpublished.

[18] E. R. Gagliano, A. G. Rojo, C. A. Balseiro, and B. Alascio, Solid State Commun. **64**, 901 (1987); C. A. Balseiro, A. G. Rojo, E. R. Gagliano, and B. Alascio, Phys. Rev. B **38**, 9315 (1988); J. E. Hirsch, S. Tang, E. Loh, Jr., and D. Scalapino, Phys. Rev. Lett. **60**, 1668 (1988); J. E. Hirsch, E. Loh, Jr., D. J. Scalapino, and S. Tang, Phys. Rev. B **39**, 243 (1989).

[19] C. A. Balseiro, M. Avignon, A. G. Rojo, and B. Alascio, Phys. Rev. Lett. **62**, 2624 (1989).

[20] R. T. Scalettar, Physica C (Amsterdam) **162**, 313 (1989); R. T. Scalettar, D. J. Scalapino, R. L. Sugar, and S. R. White (unpublished); G. Dopf, A. Muramatsu, and W. Hanke, Physica C (Amsterdam) **162**, 807 (1989); Phys. Rev. B **41**, 9264 (1990).

[21] S. Trugman, Phys. Scr. T **27**, 113 (1989).

[22] M. D. Nuñez Regueiro and A. A. Aligia, Phys. Rev. Lett. **61**, 1889 (1988).

[23] H. Castilo, C. Balseiro, B. Alascio, and H. Ceva, Phys. Rev. B **40**, 224 (1989).

[24] J. Wagner, R. Putz, G. Dopf, B. Ehlers, L. Lilly, A. Muramatsu, and W. Hanke (unpublished).

[25] P. Thiry, G. Rossi, Y. Petroff, A. Revcolevschi, and J. Jegoudez, Europhys. Lett. **5**, 55 (1988); W. A. Royer, R. J. Cava, and N. V. Smith (unpublished); D. E. Ramaker, in *Chemistry of High Temperature Superconductors II,* edited by D. L. Nelson and T. F. George (American Chemical Society, Washington, D.C., 1988), p. 84.

[26] G. D. Mahan (unpublished).

[27] Z. Tešanović, A. R. Bishop, and R. L. Martin, Solid State Commun. **68**, 337 (1988).

[28] Hirsch *et al.* (Ref. 18).

[29] This special case obtains close to half-filling if $t' \sim 0$ and $U/t \ll 1$, when there are competing instabilities in both the SDW and superconducting channels, similar to the case of a one-dimensional metal. Here the particle-particle and particle-hole channels must be treated on an equal footing (Ref. 14). This complication can be neglected in the physical parameter range.

[30] N. F. Berk and J. R. Schrieffer, Phys. Rev. Lett. **17**, 433 (1966); S. Doniach and S. Engelsberg, *ibid.* **17**, 750 (1966); W. F. Brinkman and S. Engelsberg, Phys. Rev. **169**, 417 (1968).

[31] W. R. Hanke and L. J. Sham, Phys. Rev. B **12**, 4501 (1975); S. K. Sinha, R. P. Gupta, and D. L. Price, *ibid.* **9**, 2564 (1974).

[32] J. Bang, K. Quader, E. Abrahams and P. B. Littlewood, Phys. Rev. B **42**, 4865 (1990).

[33] S. Engelsberg and J. R. Schrieffer, Phys. Rev. **131**, 993 (1963).

[34] D. J. Scalapino, E. Loh, and J. E. Hirsch, Phys. Rev. B **34**, 8190 (1986); **35**, 6694 (1987); N. E. Bickers, D.J. Scalapino, and R. T. Scalettar, Int. J. Mod. Phys. B **1**, 687 (1987).

[35] J.-M. Imer *et al.*, Phys. Rev. Lett. **62**, 336 (1989); C. G. Olson *et al.*, Science **245**, 731 (1989).

[36] P. W. Anderson, in Proceedings of the Materials Research Society Fall Meeting, November 1989 (to be published); Phys. Rev. Lett. **64**, 1839 (1990); Int. J. Mod. Phys. B **4**, 181 (1990); C. M. Varma, P. B. Littlewood, S. Schmitt-Rink, E. Abrahams, and A. E. Ruckenstein, Phys. Rev. Lett. **63**, 1996 (1989); **64**, 497 (1990)(E).

[37] S. Schmitt-Rink, C. M. Varma, and A. E. Ruckenstein, Phys. Rev. Lett. **63**, 445 (1989).

[38] F. C. Zhang and T. M. Rice, Phys. Rev. B **37**, 3759 (1988).

[39] Cohen and Louie (Ref. 8) have argued that the model interaction of Eq. (11) overemphasizes the attraction at small $q \ll k_F$. Using either a Lindhard dielectric function or a calculated ϵ for Ge, they find that the superconducting kernel is repulsive at *all* frequencies, in contrast to the model form.

[40]M. L. Cohen and P. W. Anderson, in *Superconductivity in d- and f-Band Metals* (Ref. 6), p. 17.

[41]D. A. Kirzhnits, Usp. Fiz. Nauk **119**, 357 (1976) [Sov. Phys.—Usp. **19**, 530 (1976)]; O. V. Dolgov, D. E. Kirzhnits, and E. G. Maksimov, Rev. Mod. Phys. **53**, 81 (1981); P. B. Allen, M. L. Cohen, and D. R. Penn, Phys. Rev. B **38**, 2513 (1988).

[42]S. N. Coppersmith, Phys. Rev. B **42**, 2259 (1990).

[43]Again, the difference between bare and renormalized parameters can be important. The Hartree-Fock transfer integral is reduced from the bare value by the effect of V. Hence $V/t_{\text{bare}} > V/t_{\text{HF}}$, and it is, of course, the renormalized value and not the bare value that can be compared to the band structure. S. N. Coppersmith and P. B. Littlewood, Ref. 2.

[44]W. H. Weber, C. R. Peters, B. M. Wanklyn, C. Chen, and B. E. Watts, Phys. Rev. B **38**, 917 (1988); S. Sugai, S. Shamoto, and M. Sato, *ibid.* **38**, 6436 (1988); I. Ohana, D. Heiman, M. S. Dresselhaus and P. J. Picone, *ibid.* **40**, 2225 (1989); **41**, 225 (1990).

[45]R. E. Cohen, W. E. Pickett, and H. Krakauer, Phys. Rev. Lett. **62**, 831 (1989); W. E. Pickett, Rev. Mod. Phys. **61**, 433 (1989), and private communication.

[46]S. L. Cooper, M. V. Klein, B. G. Pazol, J. P. Rice, and D. M. Ginsberg, Phys. Rev. B **37**, 5920 (1988); S. L. Cooper, F. Slakey, M. V. Klein, J. P. Rice, E. D. Bulowski, and D. M. Ginsberg, *ibid.* **38**, 12 934 (1988).

[47]S. D. Conradson and I. D. Raistrick, Science **243**, 1340 (1987).

[48]S. D. Conradson, I. D. Raistrick, and A. R. Bishop, Los Alamos National Laboratory Report No. LA-UR-89-2460 (unpublished).

[49]K. Rabe (unpublished).